Comparison of Estimated Atmospheric Boundary Layer Mixing Height in the Arctic and Southern Great Plains under Statically Stable Conditions: Experimental and Numerical Aspects

A.A. Aliabadi[1,*], R.M. Staebler[1], J. de Grandpré[2], A. Zadra[3], and P.A. Vaillancourt[3]

[1]*Atmospheric Processes Research Section, Environment Canada, Toronto, Ontario, Canada*
[2]*Atmospheric Modelling and Integration Research Section, Environment Canada, Dorval, Quebec, Canada*
[3]*Atmospheric Numerical Weather Prediction Research Section, Environment Canada, Dorval, Quebec, Canada*

[Original manuscript received 3 December 2014; accepted 8 September 2015]

ABSTRACT *The atmospheric boundary layer mixing height (MH) is an important bulk parameter in air quality (AQ) modelling. Formulating this parameter under statically stable conditions, such as in the Arctic, has historically been difficult. In an effort to improve AQ modelling capacity in North America, MH is studied in two geographically distinct areas: the Arctic (Barrow, Alaska) and the southern Great Plains (Lamont, Oklahoma). Observational data from the Atmospheric Radiation Measurement program, Climate Research Facility and numerical weather forecasting data from Environment Canada's Regional Global Environmental Multiscale (GEM15) model have been used in order to examine the suitability of available parameterizations for MH under statically stable conditions and also to compare the level of agreement between observed and modelled MH. The analysis period is 1 October 2011 to 1 October 2012. The observations alone suggest that profile methods are preferred over surface methods in defining MH under statically stable conditions. Surface methods exhibit poorer comparison statistics with observations than profile methods. In addition, the fitted constants for surface methods are site-dependent, precluding their applicability for modelling under general conditions. The comparison of observations and GEM15 MH suggests that although the agreement is acceptable in Lamont, the default model surface method contributes to a consistent overprediction of MH in Barrow in all seasons. An alternative profile method for MH is suggested based on the bulk Richardson number. This method is shown to reduce the model bias in Barrow by a factor of two without affecting model performance in Lamont.*

RÉSUMÉ [*Traduit par la rédaction*] *La hauteur de mélange de la couche limite atmosphérique représente un important paramètre général en modélisation de la qualité de l'air. La formulation de ce paramètre pour des conditions hydrostatiques stables, comme dans l'Arctique, s'est toujours avérée difficile. Afin d'améliorer la modélisation de la qualité de l'air en Amérique du Nord, nous étudions les hauteurs de mélange de deux régions géographiques distinctes : l'Arctique (Barrow, Alaska) et les grandes plaines du sud (Lamont, Oklahoma). Nous utilisons des données provenant du programme de mesure du rayonnement atmosphérique (ARM) du Climate Research Facility et des prévisions météorologiques numériques issues du Modèle global environnemental multi-échelle régional d'Environnement Canada (GEM15), afin d'examiner la pertinence des paramétrisations existantes de la hauteur de mélange, pour des conditions hydrostatiques stables. Nous comparons aussi les hauteurs observées et simulées. La période d'analyse s'étend du 1er octobre 2011 au 1er octobre 2012. Les observations à elles seules laissent penser que les méthodes fondées sur des profils sont supérieures aux méthodes limitées à la surface, en ce qui concerne la détermination de la hauteur de mélange pour des conditions hydrostatiques stables. Selon les observations, les méthodes de surface présentent des statistiques moins probantes que les méthodes avec profils. De plus, les constantes ajustées des méthodes de surface sont dépendantes du site. Elles ne peuvent donc pas s'appliquer à la modélisation de conditions générales. La comparaison entre les hauteurs de mélange observées et celles issues du GEM15 laisse penser que la méthode par défaut du modèle (surface) produit des hauteurs de mélange trop élevées à Barrow, en toute saison, bien que les données restent comparables pour Lamont. Nous suggérons donc, pour les hauteurs de mélange, une méthode avec profil, fondée sur le nombre de Richardson apparent. Cette méthode réduit par un facteur de deux le biais du modèle à Barrow, et ce, sans affecter sa performance à Lamont.*

*Corresponding author's email: aliabadi@aaa-scientists.com

KEYWORDS Arctic; boundary layer; mixing height; parameterization; profile methods; static stability; mid-latitude; surface methods

1 Introduction

Researchers have used various conventions to define and parameterize the atmospheric boundary layer or mixing height (MH). Stull (2003) defines MH as the part of the atmosphere directly influenced by the presence of the earth's surface, responding to surface forcing at a time scale less than one hour. Another definition is the height at which turbulent variances or fluxes of momentum and heat reduce to, typically, less than 10% of their value near the surface (Anderson & Neff, 2008). Because of the relative ease of temperature sounding, a popular definition is based on the shape of the vertical profile for potential temperature, where MH is the elevation with onset of the first positive slope and inversion layer aloft (Fig. 1). However, this is only a convention and should not be misunderstood as support for using this method. Alternatively, another popular definition of MH in chemistry studies is the depth at which sharp vertical gradients are observed in atmospheric constituent concentrations, such as ozone (Anderson & Neff, 2008). Yet another choice for the definition of MH is based on wind magnitude and direction; MH may be defined as the height at which winds approach geostrophic or low level jet values (Liu & Liang, 2010; Stull, 2003).

In statically stable (hereafter stable) conditions, an air parcel displaced vertically by turbulence would experience a buoyancy force pushing it back towards its starting height (Stull, 2003). In statically neutral (hereafter neutral) conditions, no buoyancy force acts on such a displaced parcel, whereas in statically unstable (hereafter unstable) conditions, the buoyancy force assists the displaced parcel in moving away from its starting height (Fig. 1). Definition of stable MHs in realistic atmospheric conditions is problematic and often controversial in the literature. Unlike MHs that occur under unstable conditions, MHs under stable conditions exhibit a number of different possible characteristics. The definition of MH based on a potential temperature profile is ambiguous because under many conditions the profile has a consistent positive slope, making the identification of the first inversion layer aloft difficult (Fig. 1). Also, with growing stability, turbulence exhibits higher intermittence. Turbulent variances and fluxes of momentum and heat may increase with height (upside down boundary layer), associated with the mid-altitude processes that generate them. In addition, the strongest turbulence aloft may be detached from the surface, generated by shear associated with a low-level jet or meandering motions. Unlike unstable boundary layers, non-local mesoscale variations such as gravity waves, drainage flows, and slope winds may become important in stable boundary layers. The influence of horizontal heterogeneity is greater on stable boundary layers, creating complex flow patterns (Mahrt, 1999; Mahrt & Vickers, 2006); for example, very localized thermals may rise in stable boundary layers. For stable boundary layers, in addition to surface turbulent fluxes, the effects of advection, subsidence, and radiative processes are equally important but are often ignored for simplicity in modelling (Mahrt & Vickers, 2006).

The mixing of trace gases by turbulence in the atmospheric boundary layer has a significant effect on species distribution (Stull, 2003). It determines tracer profiles throughout the boundary layer as well as species fluxes between the boundary layer and the free troposphere. Atmospheric mixing properties depend upon static and dynamic stabilities, which vary

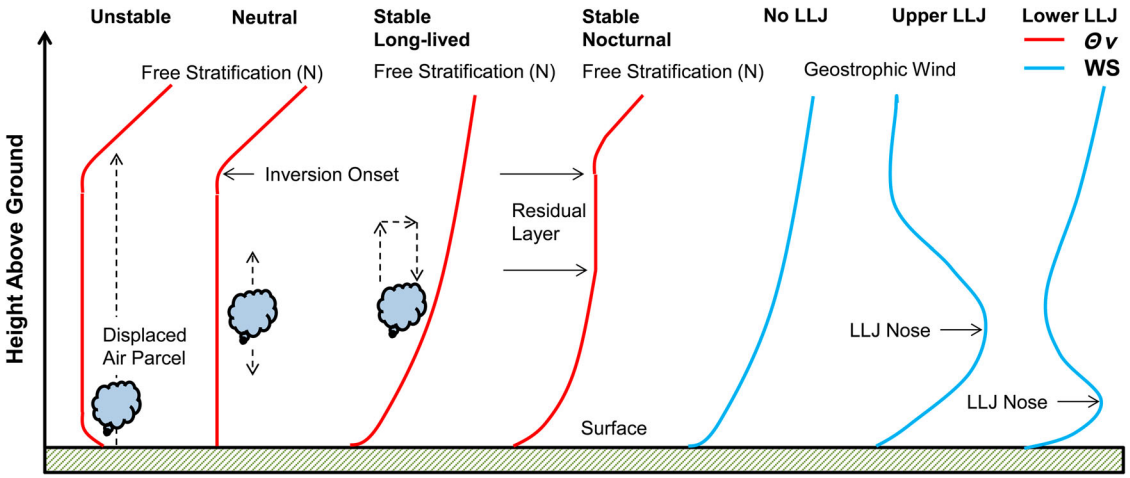

Fig. 1 Atmospheric planetary boundary layer schematic showing stable, neutral, and unstable conditions (LLJ: Low Level Jet, WS: Wind Speed, θ_v: Virtual Potential Temperature). In the unstable condition, an adiabatic parcel of air, if displaced from an original position near the surface, will accelerate upward until reaching the first inversion onset; the same parcel under neutral conditions will not accelerate; under stable cases, the parcel will experience a resisting force due to stratification pushing it back toward the original position.

significantly throughout the day, seasons, and as a function of local conditions. The parameterizations of sub-grid mixing processes by turbulence in air quality models are generally based on bulk parameters such as eddy diffusion coefficients and MH, using different formulations (Dastoor & Pudykiewicz, 1996; Han, Zhang, & An, 2009; Seibert et al., 1998). The turbulent fluxes of trace species can be influenced by MH (Holtslag & Boville, 1993); MH can also be used explicitly as a way of forcing complete mixing of constituents (Lin, Youn, Liang, & Wuebbles, 2008) or by resetting minimum eddy diffusion coefficient values within it to ensure minimum mixing, as is the case in Environment Canada's A Unified Regional Air-quality Modelling System (AURAMS; Makar et al., 2014). In all cases, the impact of MH on air quality results can be significant, which is why it is important to ensure that MH is characterized correctly in atmospheric models.

a *Objectives*

Despite decades-old research on parameterization of MH under static stability, there is still no general consensus as to which formulation to use to successfully estimate MH under general conditions. Instead, most researchers have recommended a certain formulation under a specific location or time period and, as a result, have obtained highly tuned constants to fit particular observations. To improve parameterization of atmospheric MH in numerical weather forecasting and air pollution modelling at a regional level in North America, atmospheric MH at a mid-latitude site (Lamont, Oklahoma), characterized by a weakly stable or unstable boundary layer, is compared with a high-latitude site (Barrow, Alaska), which is dominated by a strongly stable boundary layer (Fig. 2). The detailed comparison corresponds to a full year, from 1 October 2011 to 1 October 2012. A particular focus of the study is an assessment of the suitability of available parameterizations for a stable MH. Both observed and modelled results are used to answer the following questions. How do observed and modelled MH compare in mid- and high latitudes? Are observationally fitted constants for proposed MH parameterizations similar in both mid- and high latitudes? Which parameterizations for MH improve the observation–model agreement in both mid- and high latitudes simultaneously? The benefits from this comparison have wider applications in areas greatly influenced by stable conditions in the atmosphere, such as the northern latitudes during winter.

2 Methodology

a *Methods for MH Estimation*

1 STABLE MH ESTIMATION USING PROFILE METHODS

By the very definition of MH in Section 1, the most natural way to estimate MH is through profile methods. Profile methods consider the vertical profiles of turbulent fluxes, kinetic energy, atmospheric constituents, virtual potential temperature, and/or wind velocity in order to determine the equilibrium MH (h_e) (i.e., the asymptotic value which MH

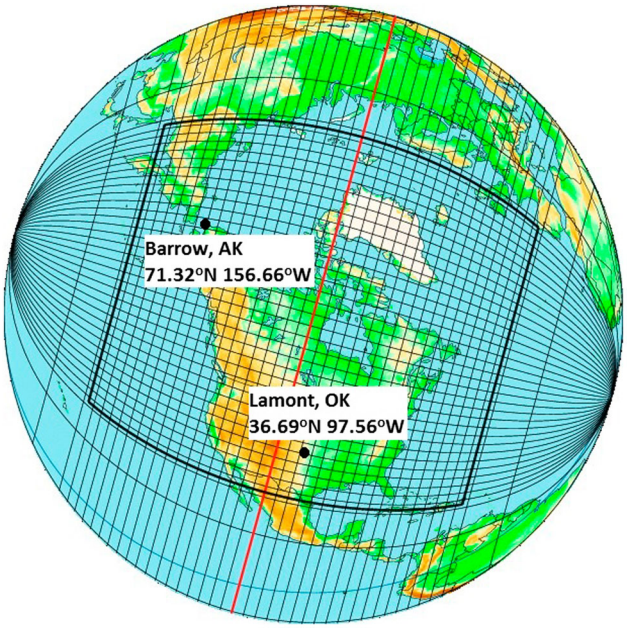

Fig. 2 Representation of Environment Canada's regional GEM15 model domain and the analysis locations of Barrow, Alaska, and Lamont, Oklahoma. The GEM15 model has a variable resolution grid with a higher constant resolution core and a decreasing resolution outside this core. In the image, every 15th grid point is shown.

approaches if boundary and initial conditions in the boundary layer were to be fixed in time). Some example methods are shown in Table 1 as MH0 to MH4. Profile methods based on atmospheric constituents, such as ozone, are particularly desired when air quality modelling is involved. A convenient way is to define MH at an elevation where the vertical gradient of ozone concentration goes above a threshold (method MH0).

The profile method of Heffter (personal communication, 1980; MH1) uses the virtual potential temperature ($\overline{\theta_v}$) gradient with criteria related to the strength of an inversion layer and the virtual potential temperature difference across the top and bottom of the layer in order to define MH. A three-point moving average is applied to a sonde profile for smoothing, and MH is taken as the middle of the lowest inversion layer in which the virtual potential temperature difference between the base and top of the layer is greater than a threshold (2 K). If this criterion is not met within the first 4 km, then the height at which the largest maximum potential temperature gradient occurs is taken as the MH.

The profile method of Liu & Liang (2010; MH2) is defined one way for the convective and neutral cases and a different way for the stable cases. In convective and neutral cases, MH is determined as the height at which an air parcel rising adiabatically from the surface becomes neutrally buoyant. For the stable regime, MH is defined at either the top of the bulk stable layer starting from the ground or at the level of the low level jet nose, if present, whichever is lower.

The profile methods of the bulk Richardson number (MH3 and MH4) are based on pioneering work by Richardson (1920). He used the laws of classical thermodynamics and

TABLE 1. Summary of MH parameterizations; profile methods have applicability under both stable and unstable conditions, whereas surface methods shall only be applied under stable conditions.

Method	Type	Reference	Description	Constants
MH0	Profile	(Stull, 2003)	$\frac{\partial O_3}{\partial z}$	Arbitrary threshold
MH1	Profile	(Heffter, personal communication, 1980)	$\Delta\overline{\theta_v}$ across inversion layer or $\frac{\partial\overline{\theta_v}}{\partial z}$	2 K across inversion layer or maximum gradient
MH2	Profile	(Liu & Liang, 2010)	Profiles of $\overline{\theta_v}$ or wind speed	Top of bulk stable layer or low level jet nose
MH3	Profile	(Mahrt, 1981)	$\mathrm{Ri_B} = \frac{h\frac{g}{\overline{\theta_{v0}}}(\overline{\theta_v} - \overline{\theta_{v0}})}{\overline{U}^2 + \overline{V}^2}$, $h_e = \frac{\mathrm{Ri_{BC}}(\overline{U}^2 + \overline{V}^2)}{\frac{g}{\overline{\theta_{v0}}}(\overline{\theta_v} - \overline{\theta_{v0}})}$	$\mathrm{Ri_{BC}} = 0.25$
				$\mathrm{Ri_{BC}} = 0.5$
MH4	Profile	(Mahrt, 1981)	$\mathrm{Ri_B} = \frac{h\frac{g}{\overline{\theta_{v0}}}(\overline{\theta_v} - \overline{\theta_{v0}})}{\overline{U}^2 + \overline{V}^2}$, $h_e = \frac{\mathrm{Ri_{BC}}(\overline{U}^2 + \overline{V}^2)}{\frac{g}{\overline{\theta_{v0}}}(\overline{\theta_v} - \overline{\theta_{v0}})}$	
MH5	Surface	(Rossby & Montgomery, 1935)	$h_e = C_n\frac{u_*}{f}$	$C_n = 0.04 - 0.5$
MH6	Surface	(Zilitinkevich, 1972)	$h_e = C_{\mathrm{sr}}\sqrt{\frac{u_* L}{f}}$	$C_{\mathrm{sr}} = 0.13 - 0.74$
MH7	Surface	(Pollard, Rhines, & Thompson, 1972)	$h_e = C_{\mathrm{ir}}\frac{u_*}{\sqrt{fN}}$	$C_{\mathrm{ir}} = 1.7$
MH8	Surface	(Deardorff, 1972)	$h_e = C_i\frac{u_*}{N}$	$C_i = 4.13$
MH9	Surface	(Zilitinkevich & Mironov, 1996)	$\left(\frac{fh_e}{C_n u_*}\right)^2 + \frac{h_e}{C_{\mathrm{sr}}}\sqrt{\frac{f}{u_* L}} = 1$	C_n, $C_{\mathrm{sr}} = 0.5$, 1.0
MH10	Surface	(Zilitinkevich et al., 2002)	$h_e = \frac{C_R u_*}{f}\left(1 + \frac{C_R^2 u_*(1 + C_{uN} LN/u_*)}{C_S^2 fL}\right)^{-1/2}$	C_R, C_{uN}, $C_S = 0.3 - 0.5$, $0.1 - 0.35$, $0.6 - 0.79$

developments by Osborne Reynolds to show that kinetic energy of eddies in the atmosphere will enhance if

$$\left(\frac{\partial\overline{U}}{\partial z}\right)^2 + \left(\frac{\partial\overline{V}}{\partial z}\right)^2 > \frac{g}{\overline{\theta_v}}\frac{\partial\overline{\theta_v}}{\partial z} \tag{1}$$

or decline otherwise, where $\overline{U}$ and $\overline{V}$ are time-averaged horizontal components of wind velocity, g the gravitational acceleration, and z the vertical coordinate. This inequality later evolved into the gradient Richardson number (Ri) that has become widely used in atmospheric physics. Later, Taylor (1935) showed that infinitesimal disturbances, in a steady state and homogeneous stably stratified sheared flow, decay if Ri exceeds a critical value (Ri_C),

$$\mathrm{Ri} = \frac{\frac{g}{\overline{\theta_v}}\frac{\partial\overline{\theta_v}}{\partial z}}{\left(\frac{\partial\overline{U}}{\partial z}\right)^2 + \left(\frac{\partial\overline{V}}{\partial z}\right)^2} > \mathrm{Ri}_C = 0.25. \tag{2}$$

The estimate for $\mathrm{Ri}_C = 0.25$ is derived from perturbation analysis. The estimate $\mathrm{Ri}_C = 0.25$ is not immediately applicable to the turbulent atmospheric boundary layer, which is always heterogeneous in the vertical space and often unsteady in time. Nevertheless, an arbitrary Ri_C has become a convenient practical tool to distinguish between the boundary layer interior, supposed to be essentially turbulent, and the free atmosphere, supposed to be essentially non-turbulent or only weakly turbulent (Zilitinkevich & Baklanov, 2002). The critical bulk Richardson number ($\mathrm{Ri_{BC}}$) method in the determination of the MH assumes that the entire boundary layer turbulence is characterized by a single length scale and a single velocity scale. The equilibrium MH is the first elevation where the value of bulk Richardson number ($\mathrm{Ri_B}$) exceeds the critical value ($\mathrm{Ri_{BC}}$) (Mahrt, 1981),

$$\mathrm{Ri_B} = \frac{h\frac{g}{\overline{\theta_{v0}}}(\overline{\theta_v} - \overline{\theta_{v0}})}{\overline{U}^2 + \overline{V}^2}, \tag{3}$$

$$h_e = \frac{\mathrm{Ri_{BC}}(\overline{U}^2 + \overline{V}^2)}{\frac{g}{\overline{\theta_{v0}}}(\overline{\theta_v} - \overline{\theta_{v0}})}, \tag{4}$$

where $\mathrm{Ri_{BC}}$ has been set from 0.25 (Holtslag, De-Bruijn, & Pan, 1990) to 7 (Maryon & Best, 1992), but values of 0.25 (MH3) or 0.5 (MH4) are more common. The time average for virtual potential temperature near the surface is $\overline{\theta_{v0}}$, customarily taken at 2 m elevation. This method can be used wherever vertical profile soundings of potential temperature and wind velocity are available.

Another method is defined for the case of models that employ K-theory (the concept of momentum and energy eddy diffusivity) in the parameterization of turbulent fluxes defining MH as the elevation at which the momentum diffusivity first drops below a certain threshold (e.g., 1 $\mathrm{m^2\ s^{-1}}$) (Jakobsen, Berge, Iversen, & Skälin, 1995). This method indirectly defines the boundary layer as a layer in which turbulent kinetic energy is above a minimum threshold (not shown in Table 1).

Some recent profile methods are based on measurement platforms other than radiosondes. Examples include acoustic sounding with a sodar (Beyrich, 1997), temperature and humidity profile sounding using microwave radiometers (Candlish, Raddatz, Asplin, & Barber, 2012), and radio

occultation refractivity or humidity profile sounding using global positioning system (GPS) satellites (Ao et al., 2012; Xie, Wu, Ao, Mannucci, & Kursinski, 2012). Each of these methods have their own specific advantages and disadvantages but will not be discussed further due to the limited scope of this analysis.

2 STABLE MH ESTIMATION USING SURFACE METHODS

Prior to the advent of profile methods in estimating stable MH, most historical developments in this field considered surface methods. With this approach, equilibrium MH (h_e) is only assumed to be a function of its "boundaries": namely surface layer variables at its bottom such as friction velocity $\left(u_* = \sqrt[4]{\overline{u'w'_0}^2 + \overline{v'w'_0}^2}\right)$ and Obukhov length $\left(L = -\overline{\theta_v} u_*^3/(\kappa g \overline{w'\theta'_{v0}})\right)$, or possibly the free atmosphere stratification on MH's top or the Brunt-Väisälä frequency $\left(N = \sqrt{g/\theta_v}\sqrt{\partial\overline{\theta_v}/\partial z}\right)$, where u', v', and w' are instantaneous wind velocity components (i.e., turbulent fluctuation from the time average, near the surface in x, y, and z coordinates), and κ is the von Karman constant (~ 0.4). The overbar $\overline{()}$ designates time average, and the subscript 0 stands for the surface layer. The friction velocity and Obukhov length are directly related to turbulent fluxes of momentum $\left(u_*^2\right)$ and sensible heat $\left(\overline{w'\theta'_{v0}}\right)$ at the surface.

With surface layer and free atmosphere variables, most MH parameterizations are derived using scaling arguments and making approximations to the Navier-Stokes equations, summarized in Table 1 as MH5 to MH10. The reader is referred to a comprehensive list of relevant parameterizations by Seibert et al. (1998), while it is sufficient to review a few popular models here, summarized in Table 1. Under neutral stability ($L \to \pm\infty$), Rossby and Montgomery (1935) proposed that the friction velocity (u_*) and the Coriolis parameter (f) are the most relevant variables governing equilibrium MH (h_e) in the steady turbulence (MH5), with constant C_n from 0.04 (Delage, 1974) to 0.5 (Mason & Thomson, 1987). Under strong stability due to surface heat flux, Zilitinkevich (1972) proposed a different approach. Using the Ekman length scale and the concept of a limiting Richardson number at the boundary layer top to estimate effective eddy viscosity, he derived the common expression of MH6, with constant C_{sr} from 0.13 (Garratt, 1982) to 0.74 (Arya, 1981).

Another approach included the effect of free atmosphere stratification, which is adjacent to the top of the boundary layer for the long-lived stable boundary layer. The reasoning behind this inclusion is that, unlike the nocturnal boundary layer, which is separated by the residual layer from the stratification aloft, long-lived stable boundary layers (e.g., the Arctic) do not exhibit residual layers and are directly adjacent to the free atmosphere (Fig. 1). Under small surface heat flux conditions, Pollard et al. (1972) used Ekman equations, the heat conservation equation, buoyancy frequency (N), and the overall Richardson number (arbitrarily assumed to be 1 for hydrodynamic instability), to derive the expression for MH7, with a constant C_{ir} of 1.7. In the limit that the background stratification is strong, Deardorff (1972) suggested that the Coriolis parameter and Obukhov length will drop out of the set of parameters that govern the equilibrium MH, arriving at MH8, with a constant C_i of 4.13 (Kitaigorodskii & Joffre, 1988).

The formulations above are limited because each is only valid for a particular type of stable boundary layer. In other words, these parameterizations provide asymptotic values for equilibrium MH under a particular situation (e.g., no surface heat flux, very strong stratification). In an effort to overcome this difficulty, researchers have interpolated between two or more of the above limiting cases and arrived at more complex or implicit formulations that would potentially cover a wider range of static stability (e.g., from neutral to very stable). Zilitinkevich and Mironov (1996) proposed a multi-limit approach to account for intermediate regimes, arriving at MH9, with constants suggested as follows: $C_n = 0.5$ and $C_{sr} = 1.0$. (Note: three original terms associated with this model have been omitted because they were insignificant in the following analysis.) The reader must note that the constants for this interpolated scheme should not necessarily be in the same range of values as the constants reported earlier for asymptotic schemes. Zilitinkevich and Mironov (1996) warn, however, that these constants are only orders of magnitude and potentially interdependent. Another interpolation scheme was provided by Zilitinkevich et al. (2002), in which an explicit function was provided (MH10), with constants suggested as follows: $C_R = 0.3 - 0.5$, $C_S = 0.6 - 0.79$, and $C_{uN} = 0.1 - 0.35$.

Most interpolated schemes are shown to improve the estimates for the equilibrium MH over the asymptotic formulations. However, the comparisons with observations so far have only been made for a limited number of sites. Another challenge is that there is no universal agreement on what the constants should be in any of the asymptotic or interpolated formulations. The constants are often seen to be interdependent, with specific values fitted for particular observations. Furthermore, even for a single location, stable MH exhibits diurnal and seasonal variations (e.g., from very stable to weakly stable) so that conditions for many asymptotic formulations may be met at different times. This results in some asymptotic formulations performing better than others, depending on performance within or outside stability limits, for which a particular formulation was developed.

3 DIAGNOSTIC VERSUS PROGNOSTIC METHODS

All parameterizations provided in the previous section were diagnostic as opposed to prognostic, suggesting what the equilibrium MH is at any particular time and location. Researchers have suggested that the actual MH will not be equal to the equilibrium MH but will tend toward it, given that the boundary conditions affecting the MH do not change. Stull (2003)

and Mahrt (1981) have suggested an exponential relaxation for MH given an equilibrium MH:

$$h(t) = h_e + (h_0 - h_e)e^{-t/\tau_R}, \tag{5}$$

where $h(t)$ is the prognostic MH, h_e the equilibrium MH, h_0 the latest estimate of MH in the last time step, and τ_R the response time for the effects of turbulence on the entire boundary layer. For a stable boundary layer it has been suggested that τ_R ranges from 7 to 30 h (Stull, 2003). Surridge and Swanepoel (1987) have proposed a prognostic MH growth model, applicable to the nocturnal boundary layer as it develops:

$$h(t) = h_e \text{erf}\,(t/\tau_R), \tag{6}$$

where erf() is the error function. Zilitinkevich et al. (2002) proposed another prognostic model that takes into account subsidence in addition to allowing for MH growth and decay:

$$\frac{\partial h(t)}{\partial t} = w_h - C_E|f|(h - h_e), \tag{7}$$

where w_h is subsidence, and C_E is a constant suggested to be 1. This model was shown to work for an observational campaign over the Greenland ice sheets (Zilitinkevich et al., 2002).

b *Numerical Methodology*

For this study, the output of the 2011–2012 version of the operational numerical weather prediction model (the Global Environmental multiscale model hereafter referred to as GEM15) for short-range forecasts (up to 48 h) from the Canadian Meteorological Centre was used. In 2009, this regional version of the global environmental multi-scale (GEM) model had a 15 km horizontal grid spacing, shown in Fig. 2, a time step of 450 s, and 58 vertical levels extending from the surface to about 10 hPa or 26 km. The initial conditions at 0000 and 1200 UTC were provided by a regional data assimilation system based on a three-dimensional variational technique (Laroche, Gauthier, St-James, & Morneau, 1999). A description of the GEM15 physical parameterizations is given in Mailhot et al. (2006) with the exception of the radiative transfer scheme of Li and Barker (2005), which was implemented in early 2009. In particular, details on the boundary layer parameterization are found in Mailhot et al. (1998) and references therein. Since 2009, this model has undergone several upgrades in horizontal spatial resolution, data assimilation (Tanguay, Fillion, Lapalme, & Lajoie, 2012), and implementation of Richardson number hysteresis (McTaggart-Cowan & Zadra, 2015). Although these various changes have had major impacts on the meteorological performance of the regional forecasting system, they do not affect MH calculation directly, and it is believed that the results and conclusions presented in this paper also apply to the present day operational model.

The MH parameterization in GEM15 is fully described by Mailhot et al. (1998) but a short introduction is necessary here. The stability condition of the boundary layer is decided by the sign of the bulk Richardson number (i.e., $\text{Ri}_\text{B} < 0$ for unstable and $\text{Ri}_\text{B} \geq 0$ for stable conditions). The Ri_B is calculated in the surface layer, that is, the layer of the atmosphere between the actual surface and the first prognostic level of the model, which in the case of GEM15 is approximately 40 m above the surface. Because the model uses hybrid vertical coordinates, the actual height of the first prognostic level is flow and pressure dependent and thus varies slightly with time. The equilibrium stable MH is calculated based on surface properties using,

$$h_e = \max(h_1, h_2, h_3), \tag{8}$$

where $h_1 = 1.2(z_u + 10z_{0,m})$ with z_u being the height of model's lowest prognostic level and $z_{0,m}$ being the roughness length for momentum; $h_2 = L$, introduced earlier in Section 2.a.2, and $h_3 = \sqrt{u_* L/f}$ introduced earlier in Table 1 ($C_\text{sr} = 1$). For unstable cases, the equilibrium MH is calculated based on either surface properties or profile methods using,

$$h_e = \max(h_4, h_5), \tag{9}$$

where $h_4 = 0.3u_*/f$ introduced earlier in Table 1 ($C_n = 0.3$), and h_5 is the lowest level where the gradient of virtual potential temperature $\partial\overline{\theta_v}/\partial z$ is positive, similar to the profile method of Heffter (personal communication, 1980).

The surface scheme in GEM15 considers four types of surfaces: land, water, sea ice, and glaciers, each controlled by a separate scheme. For each grid cell of the model, the surface is partitioned into these types. For Lamont, it is 100% land, whereas for Barrow it is 82% water or sea ice depending on season, 17% tundra, and 1% glacier. There is a separate calculation of surface fluxes and parameters for each type of surface. For a grid cell, the final values of surface momentum and sensible heat fluxes (as well as the final values of h_e, L, z_0, and surface meteorological variables) are obtained by aggregation (i.e., a weighted average). In summary, if the grid cell of interest is a complex mix of different types of surfaces, then the value of h_e is a combination of separate estimates.

Unlike equilibrium MH (h_e), the real-time MH (h) in boundary-layer modelling is calculated using a predefined function. In GEM15 the MH approaches this equilibrium value either with step change or exponentially,

$$h = \begin{cases} h_e & \text{if} \quad h_e \geq h_0 \\ h_e + (h_0 - h_e)e^{-\Delta t/\tau} & \text{if} \quad h_e < h_0 \end{cases}$$

Although MH decay is modelled exponentially according to the methods of Stull (2003) and Mahrt (1981), MH growth is modelled with step changes. The relaxation constant (τ) is taken as 1.5 h, much shorter than the recommendation of Stull (2003) (>7 h). Under stable cases, the value of h is

limited to the range [30, 1500] m, but under unstable conditions if the lowest level positive gradient in virtual potential temperature is greater than 1500 m, then MH can be greater than 1500 m.

The unstable MH is a purely diagnostic variable in GEM15 and not expected to alter other variables. Stable MH, however, weakly affects the surface stability functions, which in turn alters other variables slightly. Although mainly diagnostic in meteorology, MH is used in a prognostic manner in many chemical transport models as mentioned in Section 1, so its parameterization significantly affects AQ models.

c *Observational Data*

The experimental stations were located in Lamont, Oklahoma (36.69°N 97.56°W) and Barrow, Alaska (71.32°N 156.66° W). Both locations have relatively flat terrains. For both sites, value-added products (VAP) from the Atmospheric Radiation Measurement (ARM) program, Climate Research Facility, US Department of Energy, were used to provide merged profiles of potential temperature, wind speed, and wind direction. The merged sounding VAP uses a combination of observations from several different platforms (e.g., radiosondes, profiling microwave radiometers, surface-based meteorology measurements), output from computer model simulations of atmospheric conditions (e.g., European Centre for Medium-range Weather Forecasts (ECMWF)), and a sophisticated scaling/interpolation/smoothing scheme in order to define profiles of the atmospheric thermodynamic state at a high time resolution (https://www.arm.gov/data/vaps). In addition, the MH based on the profile methods of Heffter (personal communication, 1980; MH1), Liu and Liang (2010; MH2), and Mahrt (1981; MH3 and MH4) were obtained from ARM for both sites. The MHs at Barrow are available twice daily, and in Lamont there are four measurements per day.

Quality-controlled eddy covariance flux measurements and surface meteorological data were obtained from ARM. Operation of the Eddy CORrelation (ECOR) flux measurement system is based on the eddy covariance technique. The uncertainties for flux estimates by ECOR are 6% for sensible heat flux and 5% for momentum flux (https:www.arm.gov/instruments/ecor). The data included 30 m averages for friction velocity, sensible heat flux, mixing ratio, relative humidity, pressure, temperature, wind speed, wind direction, air density, and air specific heat capacity.

To benchmark a reference MH, ozonesondes were launched twice daily on consecutive days from Barrow at approximately 0600 and 1800 local time for a total of 28 launches in April 2009. This enabled the measurement of vertical concentration profiles with a resolution of 10 m or better (Helmig et al., 2012).

d *Statistical Methodology*

1 COMPARISON OF TWO SAMPLE VARIABLES

Point-by-point comparison of two sample variables is performed using the bias and root mean square (RMS) error statistics. If the two sample variables of interest are X and Y, the bias and RMS error can be computed by the mean and standard deviation of the difference sample variable $X - Y$.

2 MODEL FITTING

A genetic optimization algorithm is used to fit one or more constants associated with different MH models of interest efficiently. In this technique, a starting guess for the constants are provided. Subsequently, four parameters are set to specify how the genetic optimization is initialized and proceeds. These are iterations, population size, mutation constant, and recombination constant, which are set to 200, 20, 0.7, and 0.5, respectively in this analysis. In this method, a global cost function is minimized,

$$\chi^2 = \sum_{i=1}^{n} \frac{(Y_i - X_i)^2}{S_X}, \tag{10}$$

where Y is the modelled sample variable, X is the observed sample variable, and S_X is the observed sample standard error. With units of metres, χ^2 usually grows with degrees of freedom $\nu = n - 1$. This technique provides a fast converged solution, but it does not necessarily find a global minimum, as otherwise would be found by an entire phase-space search (Wormington, Panaccione, Matney, & Bowen, 1999).

3 Results and discussion

a *Suitable Profile Diagnostics for Mixing Height*

A suitable diagnostic for MH is not unique because it depends on the way MH is defined. For example, if reduction of turbulent fluxes or kinetic energy to 10% of their near-surface values is used to define MH, then turbulence profile measurements are needed to diagnose MH. These measurements are not usually available. With this definition, MH is particularly more difficult to identify, and there is no algorithm to determine the stable boundary layer top accurately without actual observations of the turbulent kinetic energy profile (Stull, 2003).

From the perspective of AQ modelling, the use of vertical tracer profiles is a suitable diagnostic for MH. Profiles of concentration should exhibit large gradients at the MH top due to turbulence. Figure 3 shows profiles of ozone at Barrow as a means of determining MH based on atmospheric constituents. In this method, a threshold of 0.04 ppb m^{-1} is used for the vertical gradient of ozone concentration (dO_3/dz) to determine the MH. Under weakly stable or neutral conditions the profile only exhibits one sharp gradient, but under very stable conditions multiple sharp gradients are observed. Under the very stable case, the sensitivity of MH determination on the threshold value is high.

In our study, availability of profile ozone data was limited to 28 ozonesonde launches in Barrow. As a result, this method (MH0) was compared with other profile methods of Heffter (personal communication, 1980; MH1), Liu and Liang

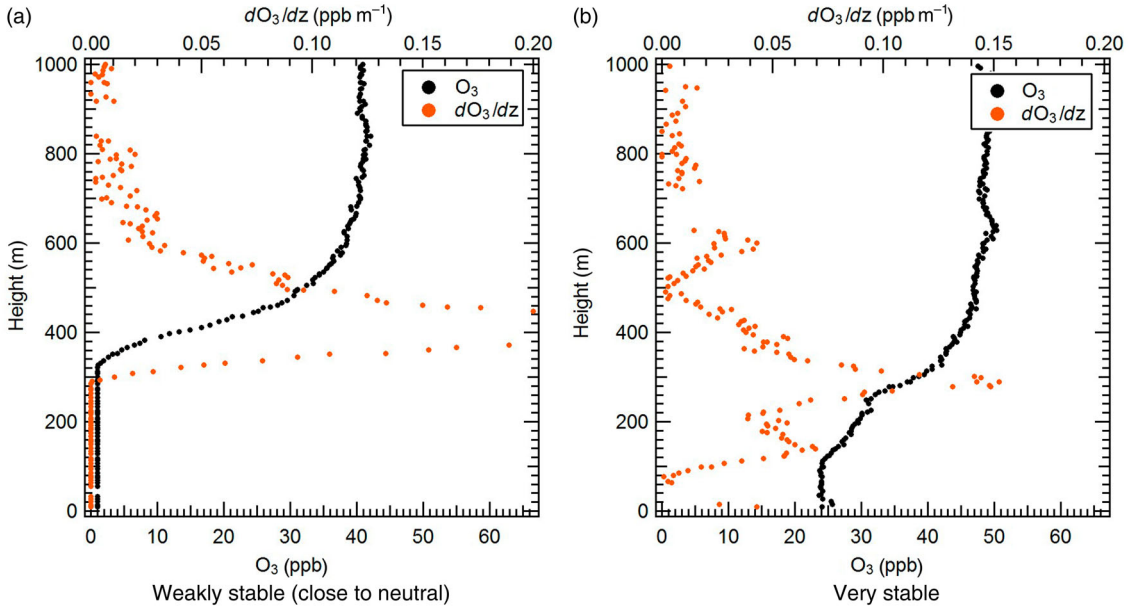

Fig. 3 MH based on ozonesonde profiles at Barrow; (a) under weakly stable or neutral conditions, the mixing degree is higher so that the concentration profile exhibits a distinguishable sharp gradient near the top of the boundary layer, whereas (b) under strongly stable conditions, multiple sharp gradients of various magnitude may be observed.

TABLE 2. Bias and RMS error between profile methods and the reference method (MH0) for MH; bias and RMS error computed for sample variable $x-$MH0, where x assumes values from MH1 to MH4 ($n = 28$).

Method	Bias (m)	RMS Error (m)
MH1	−122	225
MH2	−146	237
MH3	−141	209
MH4	−88	169

(2010; MH2), and Mahrt (1981; MH3 for $\mathrm{Ri_{BC}} = 0.25$ and MH4 for $\mathrm{Ri_{BC}} = 0.5$) to see if any of these methods provides another suitable diagnostic for the estimation of MH. Note that surface methods were not considered for this purpose because MH, by its very definition, is a profile property. The computed statistics for this comparison are provided in Table 2. Based on these comparisons we selected the method of Mahrt (1981) ($\mathrm{Ri_{BC}} = 0.5$; MH4) as the most appropriate available diagnostic, or in other words intermediate diagnostic as a benchmark for the ozone profiles, for the MH in the following analyses. The appropriateness of this selection is evident by the lowest bias and RMS error compared with other choices. In addition, Seibert et al. (2000) and Vogelezang and Holtslag (1996) recommend this method, particularly under stable conditions.

A comparison can be made among profile methods of MH1 to MH4 in Fig. 4 using the vertical profiles of virtual potential temperature and wind speed for a few example profiles. These methods generally have a one-to-one relationship. The agreement among MH1, MH2, MH3, and MH4 in determining MH is close for unstable conditions, whereas there is a spread under stable conditions.

b *Mixing Height Based on Parameterizations*

1 FITTING SURFACE PARAMETERIZATIONS BASED ON OBSERVATIONS

The surface parameterizations MH5 to MH10 described in Section 2.a.2, were used to fit constants producing the MH that was known a priori based on the observations. For parameterizations that required buoyancy frequency (N), we calculated the vertical potential temperature gradient at an elevation above the observed MH.

Table 3 shows the fitted constants and the minimized cost function $\chi^2 = \sum_{i=1}^{n} (Y_i - X_i)^2/S_X$, normalized by degrees of freedom, for the MH parameterizations. The comparative value of this cost function indicates which parameterizations result in a better fit.

For Lamont, the best fit is achieved for parameterization of MH5 or those interpolated schemes that are designed to reduce to it under close-to-neutral conditions (i.e., MH9 and MH10). More importantly, the fit constants associated with the term u_*/f (i.e., C_n and C_R) are all found to be 0.27. The other constants in the interpolated schemes (i.e., C_{sr}, C_{uN}, and C_S) adjust themselves to either maximum or minimum limits to make the contribution of other terms minimal. For Barrow, the best performance is achieved by interpolated parameterizations of MH9 and MH10. The values of the constants obtained for Lamont and Barrow differ significantly, indicating that these surface methods need to be adjusted for different sites or climatic conditions.

Figure 5 shows the scatterplots for MH estimations based on surface methods versus MH4, with $\mathrm{Ri_{BC}} = 0.5$ as justified earlier. Only stable conditions (i.e., $L > 0$) are considered in these plots. Table 4 shows the corresponding comparison statistics. For Lamont, in agreement

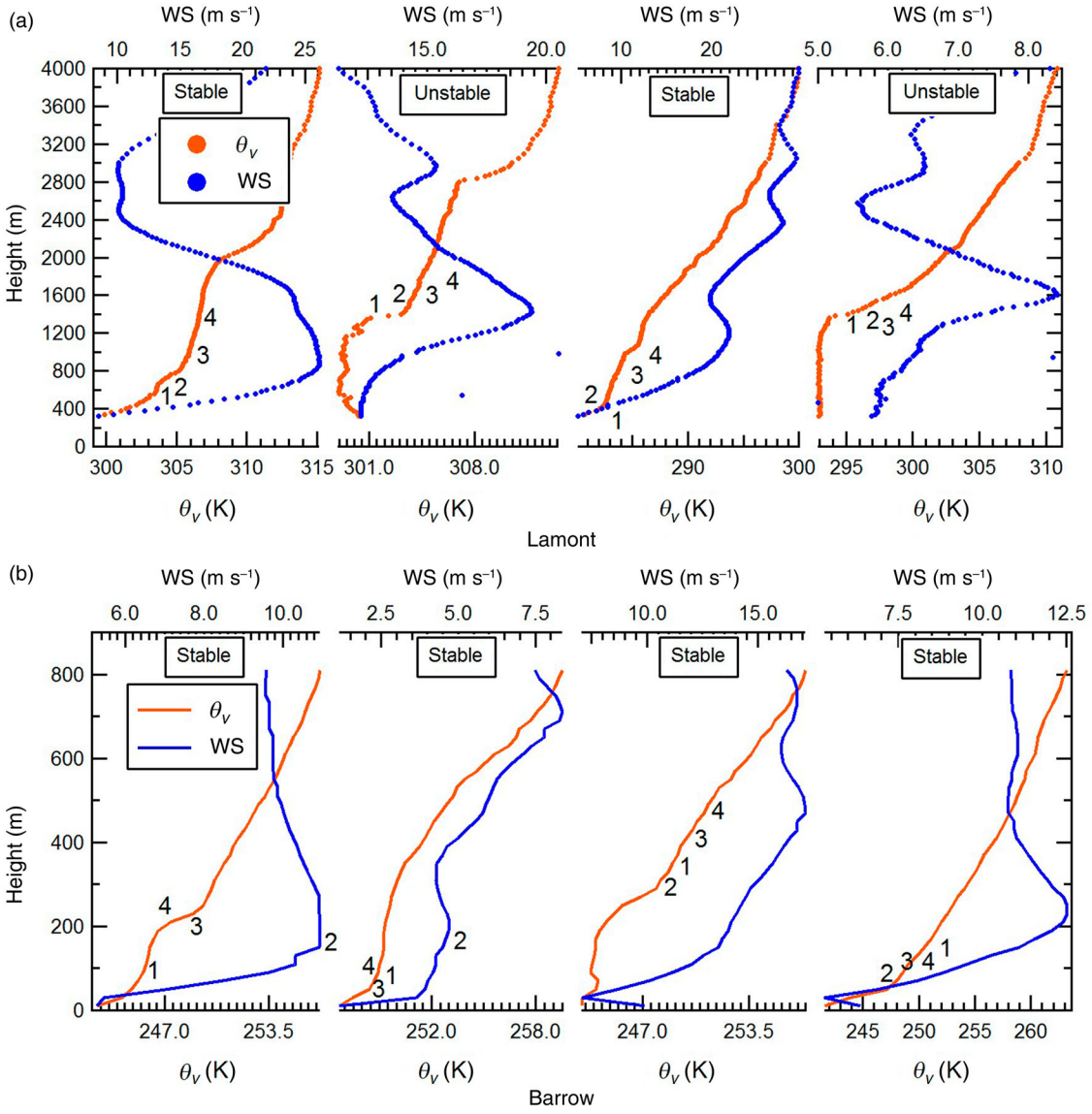

Fig. 4 MH based on profile methods MH1 to MH4 (abbreviated as 1 to 4 on graph) for selected profiles of virtual potential temperature and wind speed under all stability conditions; the agreement among methods is higher under unstable condition, whereas under stable condition, there is a higher spread among various methods.

TABLE 3. Goodness of fit and fitted constants for surface parameterizations of MH based on observations (MH4); for Lamont $\nu = n - 1 = 795$, and for Barrow $\nu = n - 1 = 131$.

Method	Lamont χ^2/ν (m)	Lamont Fitted Constants	Barrow χ^2/ν (m)	Barrow Fitted Constants
MH5	690	$C_n = 0.27$	310	$C_n = 0.14$
MH6	2000	$C_{sr} = 0.63$	400	$C_{sr} = 0.20$
MH7	810	$C_{ir} = 2.70$	320	$C_{ir} = 1.18$
MH8	1400	$C_i = 20.70$	370	$C_i = 9.12$
MH9	690	C_n, $C_{sr} = 0.27$, 1000	210	C_n, $C_{sr} = 0.40$, 0.78
MH10	650	C_R, C_{uN}, $C_S = 0.27$, 0, 1000	190	C_R, C_{uN}, $C_S = 0.33$, 0, 0.73

with Table 3, MH5, MH9, and MH10 exhibit lower biases and RMS errors. For Barrow, again in agreement with Table 3, MH9 and MH10 exhibit lower biases and RMS errors.

2 COMPARISON OF MODELLED AND OBSERVED MIXING HEIGHT

The model MHs (MHA to MHF) are formulated in Table 5. The calculations are based on a variety of techniques, all of which use model variables for derivation. MHA is based on

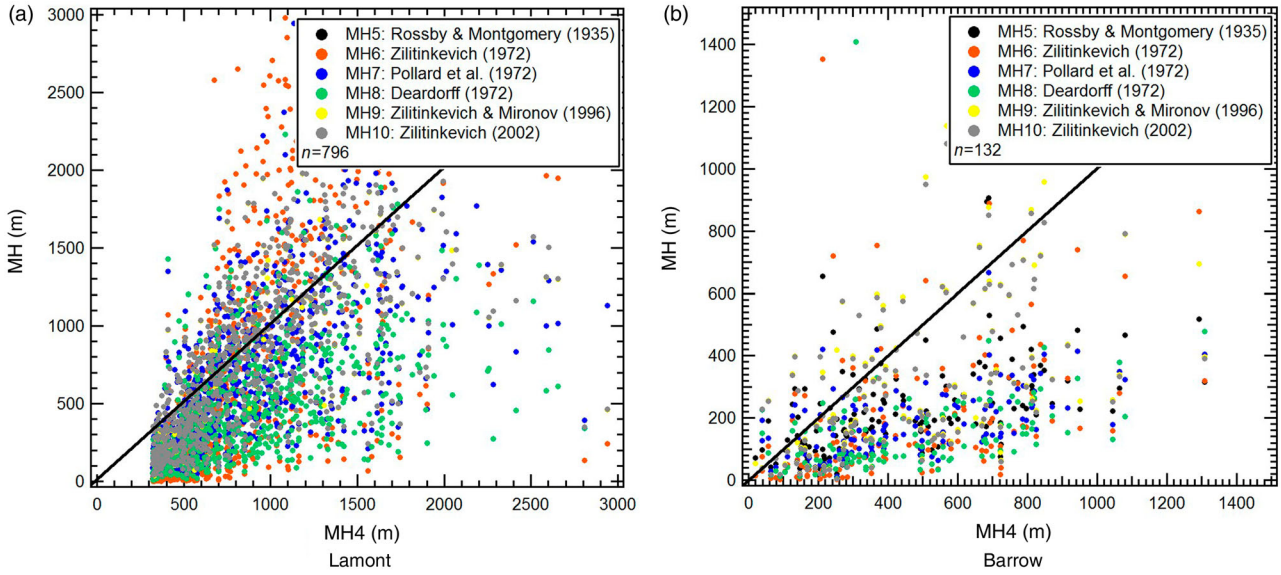

Fig. 5 Observed parameterizations of MH based on surface methods (only under stable conditions).

TABLE 4. Bias and RMS error between surface methods and MH4; bias and RMS error computed for sample variable $x-$MH4, where x assumes values from MH5 to MH10; for Lamont $n = 796$, and for Barrow $n = 132$.

Method	Lamont Bias (m)	Lamont RMS Error (m)	Barrow Bias (m)	Barrow RMS Error (m)
MH5	−122	445	−210	396
MH6	100	1070	−24	1817
MH7	−185	499	−249	407
MH8	−359	664	−293	432
MH9	−122	445	−139	321
MH10	−122	449	−137	310

the profile method of Mahrt (1981) with $\mathrm{Ri_{BC}} = 0.5$ where $\overline{\theta_{v0}}$ is taken at the first prognostic elevation of about 40 m. This choice has confirmed better results and is also justified by Mahrt (1981) who argues that the choice merely imposes an offset to the value of $\mathrm{Ri_{BC}}$, while this convention excludes any modelling errors in surface temperature in the estimation of the MH. MHB is directly available in the archived output of the model, which is based on the parameterization in Section 2.b, and MHC is based on the method of Jakobsen et al. (1995) with a threshold momentum diffusivity of $K_m = 1\ \mathrm{m^2\ s^{-1}}$. This method is chosen because GEM15 is an eddy viscosity model with momentum diffusivity available for parameterization of MH. MHD and MHF, only considered for stable conditions, are based on the formulation of Zilitinkevich (1972) in Table 1 with values of C_{sr} that are set to 1 or the fitted equivalents in Table 3 using the observations. This formulation is selected because of its wide usage in models, including GEM15. Finally, MHE, also only considered for stable conditions, is based on the formulation of Rossby and Montgomery (1935) in Table 1 and a value of C_n based on the fitted equivalents in Table 3 using the observations. This formulation, again, is singled out because of wide usage in various models.

Figure 6 and Table 6 show scatterplots and comparison statistics, respectively, for the modelled parameterizations of MH. For Lamont, a low bias and RMS error are achieved (−117 m, 521 m) using MHA. The standard GEM15 parameterization of MHB also performs well (−102 m, 565 m) because it is designed for mid-latitude climate conditions, with the exception that it is clipped at 1500 m under stable conditions as

TABLE 5. Summary of model MH parameterizations; profile methods have applicability under both unstable and stable cases, whereas surface methods are only applied under stable cases.

Method	Type	Reference	Description	Constants
MHA	Profile	(Mahrt, 1981)	$\mathrm{Ri_B} = \frac{h\frac{g}{\theta_{v0}}(\overline{\theta_v} - \overline{\theta_{v0}})}{\overline{U}^2 + \overline{V}^2}$, $h_e = \frac{\mathrm{Ri_{BC}}(\overline{U}^2 + \overline{V}^2)}{\frac{g}{\theta_{v0}}(\overline{\theta_v} - \overline{\theta_{v0}})}$	$\mathrm{Ri_{BC}} = 0.5$
MHB	Surface	GEM15 Model	Section 2.b	—
MHC	Profile	(Jakobsen et al., 1995)	K_m	$1\ \mathrm{m^2\ s^{-1}}$ threshold
MHD	Surface	(Zilitinkevich, 1972)	$h_e = C_{\mathrm{sr}}\sqrt{\frac{u_* L}{f}}$	$C_{\mathrm{sr}} = 1$
MHE	Surface	(Rossby & Montgomery, 1935)	$h_e = C_n \frac{u_*}{f}$	C_n fitted with observations
MHF	Surface	(Zilitinkevich, 1972)	$h_e = C_{\mathrm{sr}}\sqrt{\frac{u_* L}{f}}$	C_{sr} fitted with observations

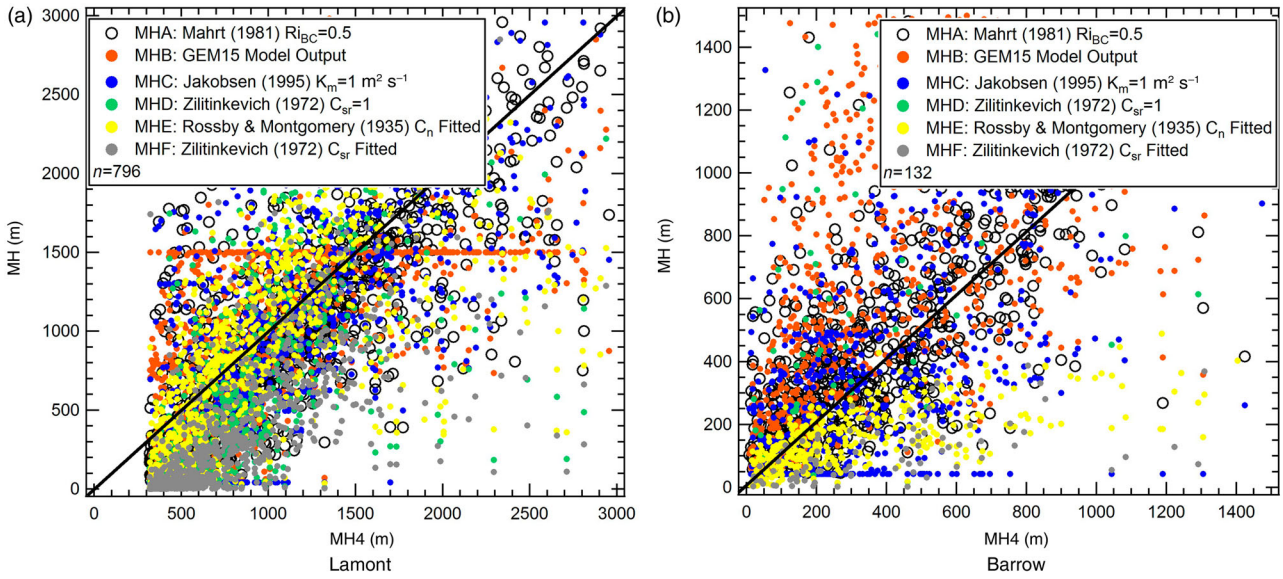

Fig. 6 Modelled parameterizations of MH; profile methods MHA and MHC apply to both stable and unstable conditions; the surface methods MHB, MHD, MHE, and MHF apply only under stable conditions.

TABLE 6. Bias and RMS error between modelled MHs and MH4; bias and RMS error computed for sample variable $x-$MH4, where x assumes values from MHA to MHF; for Lamont $n = 796$, and for Barrow $n = 132$.

Method	Lamont Bias (m)	Lamont RMS Error (m)	Barrow Bias (m)	Barrow RMS Error (m)
MHA	−117	521	68	282
MHB	−102	565	236	461
MHC	6	830	39	412
MHD	−82	1072	530	860
MHE	−116	568	−188	341
MHF	−418	757	−310	448

explained in Section 2.b. The statistics for MHC and MHD are poorer (6 m, 830 m) and (−82 m, 1072 m), respectively. The performance of MHE is better than MHD (−116 m, 568 m). The performance of MHF is poor (−418 m, 757 m).

For Barrow, MHA achieves a low bias and RMS error (68 m, 282 m). The performance of MHB is poor (236 m, 461 m), but MHC shows improved performance compared with MHB (39 m, 412 m). The poorest performance is seen with MHD (530 m, 860 m), but MHE shows improved statistics compared with MHB and MHD (−188 m, 341 m). The performance of MHF is slightly better than MHD because of the adjusted fit constant (−310 m, 448 m).

These comparisons suggest that MHA can most consistently model the observed MH given a unique constant, $Ri_{BC} = 0.5$, whereas the performance statistics of other surface parameterizations, even with adjusted constants, are still not as good as those for MHA.

To illustrate the differences in MH parameterization under mid-latitude and high-latitude climates, example MH time series are shown in Fig. 7 for the month of April (diurnal variation of MH in different seasons will be shown in the next section). The observed profile methods (MH1 to MH4) and the modelled profile methods (MHA and MHC) include all stability conditions, but MHB, MHD, MHE, and MHF only represent stable conditions per model definition in Section 2.b, (i.e., $Ri_B \geq 0$).

In Lamont, MHB is clipped at 1500 m for stable conditions as explained in Section 2.b, whereas MHs based on other formulations extend this limit. A large scatter is exhibited by MHD, while MHF exhibits a negative bias, as investigated earlier. In Barrow, MHB is clearly biased by overprediction and shows unphysical oscillations. A large positive bias is also exhibited by MHD, as expected because MHB reduces to it under specific conditions explained in Section 2.b. To the contrary, profile MHs such as MHA and MHC do not exhibit as large biases or high oscillations as in MHB. MHE, based on the fitted surface method, shows improved performance, whereas MHF, although using a fitted constant, exhibits poorer agreement with a negative bias.

Visual comparison of the above time series suggests that the surface methods significantly deviate from observations at high latitudes, particularly if their constants are not adjusted based on observations, whereas profile methods have a more consistent performance.

c *Diurnal Variation of Mixing Height in Different Seasons*

The effect of seasonal variations on model parameterizations of MH is quantified by plotting diurnal MH for selected methods, mainly the standard surface method of MHB in the GEM15 model, the suggested profile method of MHA, and the observed profile method of MH4. The results are shown in Fig. 8. For Lamont there are four observations per day, corresponding to the sonde launches, while in Barrow there are only two observations per day. For Lamont, both MHA and MHB agree well with MH4, although MHA exhibits a

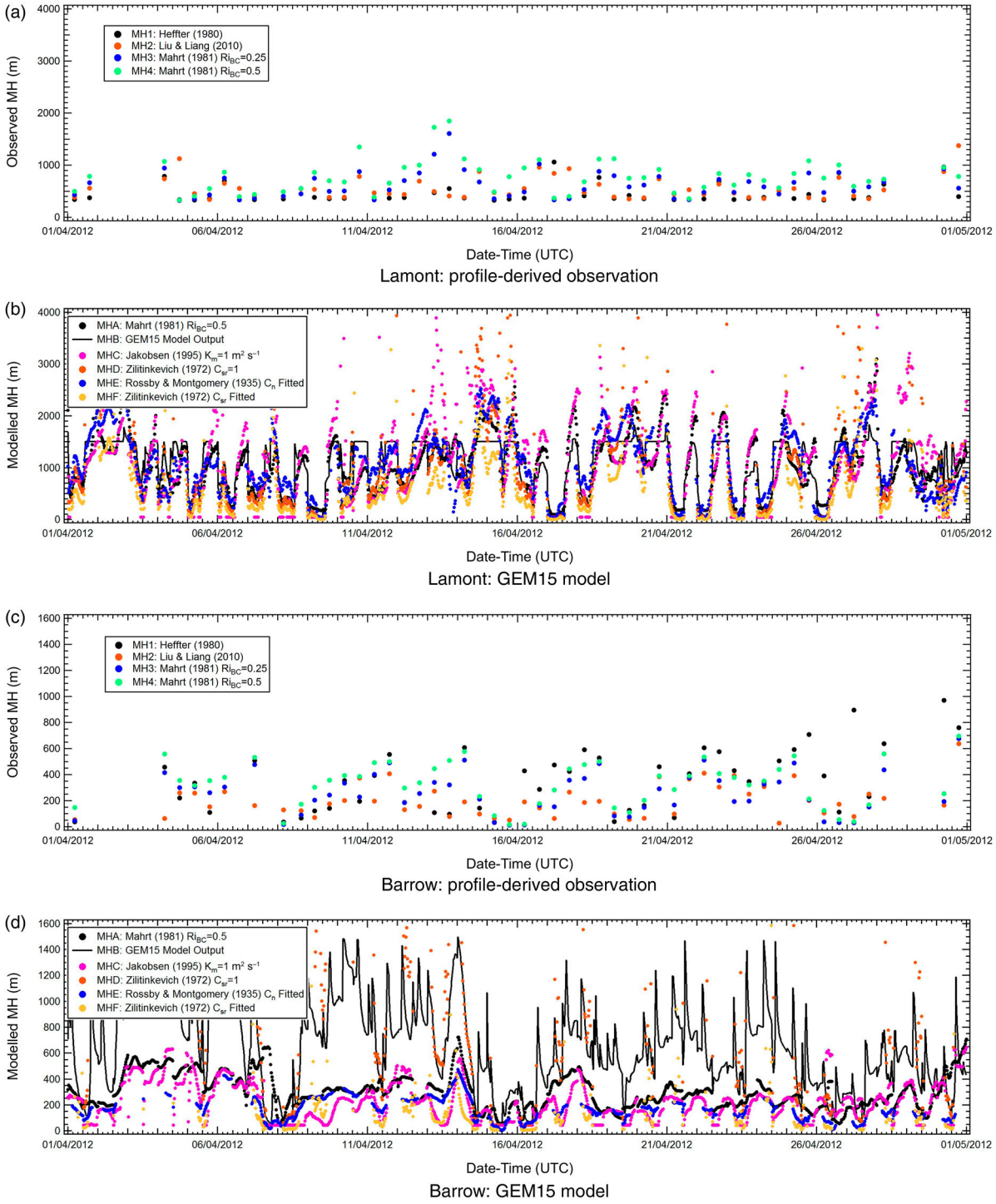

Fig. 7 Example MH time series for profile observations and model parameterizations for April 2012; profile methods MH1, MH2, MH3, MH4, MHA and MHC apply to all stability conditions; surface methods MHB, MHD, MHE, and MHF apply only under stable conditions.

marginally lower overall bias. In Barrow, however, MHB consistently exhibits a large positive bias compared with MHA. Particularly in winter (December, January, and March), MHB exhibits a large bias of up to 450 m, whereas MHA performs much better with a reduced bias of under 200 m. During spring (March, April, and May) and summer (June, July, and August), MHB still exhibits a positive bias of 400 m and 150 m, respectively, whereas MHA exhibits almost no bias. For the fall (September, October, and November), both methods exhibit a bias, although not as severely as in winter and spring. The diurnal and seasonal analysis for MH confirms that, with the choice of parameterization only, it is possible to reduce GEM15 model biases by a factor of two using MHA.

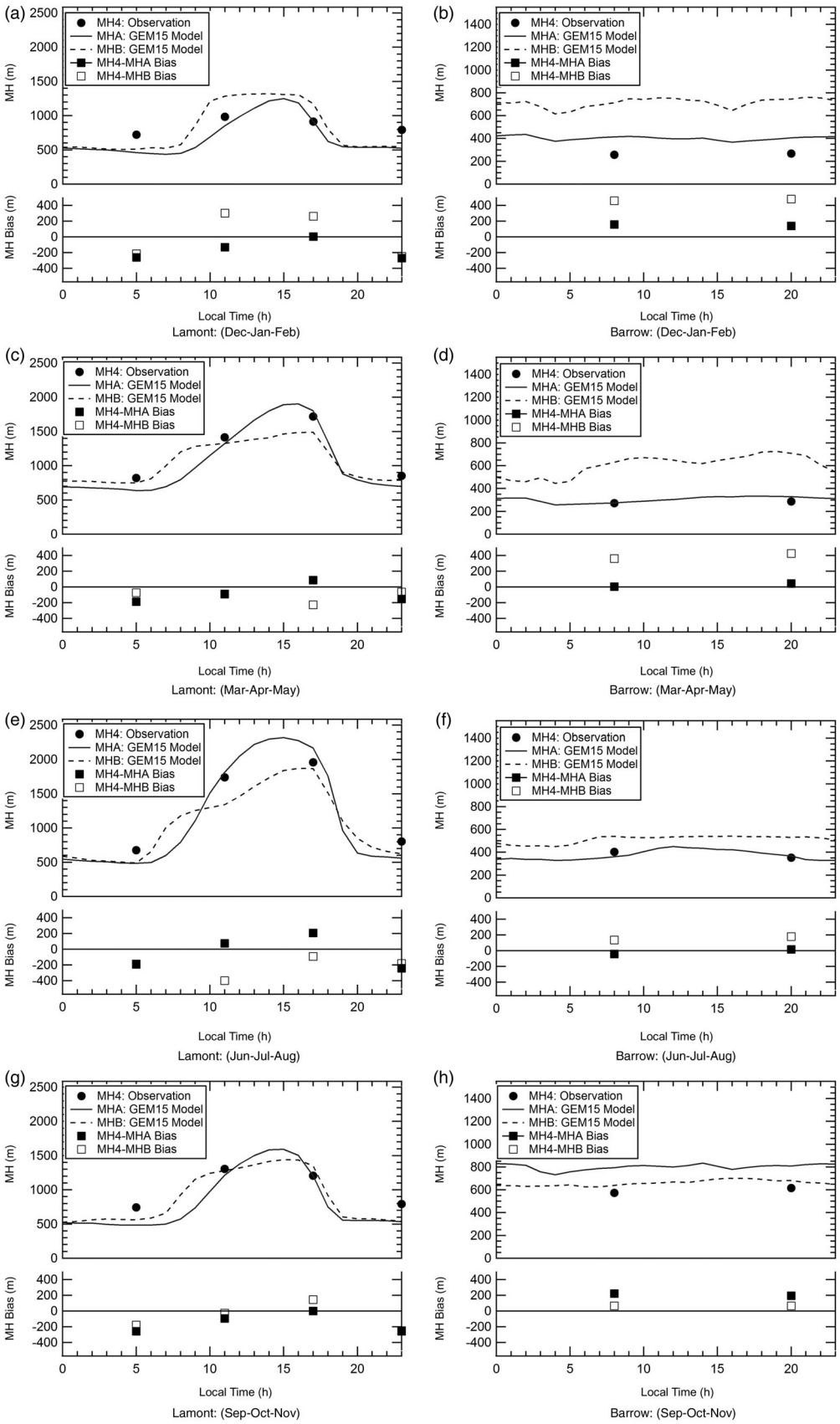

Fig. 8 Diurnal variation of MH in different seasons; average values provided for MH from ARM's observations and GEM15 model. For Lamont, four observations are available per day corresponding to four sonde launches, whereas in Barrow only two observations per day are available.

4 Conclusions and future work

Atmospheric MH in the southern Great Plains and the Arctic was studied using observations from ARM and Environment Canada's GEM15 regional weather forecasting model. One mid-latitude site (Lamont, Oklahoma) and one high-latitude site (Barrow, Alaska) were considered for a one-year analysis period from 1 October 2011 to 1 October 2012. The parameterizations available to estimate MH were those based on surface properties or profile methods. The particular focus of this study was to investigate parameterization of equilibrium MH under stable conditions at high latitudes (particularly in the Arctic), which has been historically difficult to formulate. Observed profile methods based on ozone concentration and meteorology (sondes) were used as benchmarks to examine various MH parameterizations based on both surface or profile properties.

Based on observations, stable MH estimations using surface methods were sensitive to the choice of parameterization and site location. The fitted constants for all such parameterizations were site-dependent. In Lamont, those asymptotic formulations based on neutral conditions or those interpolated schemes that reduced to this limit, performed better in predicting the observations. In Barrow, the interpolated schemes based on neutral conditions, stable conditions, and free atmosphere stratification performed better than the asymptotic formulations. Nevertheless, all pairs of fitted constants were different in the two locations.

The standard MH (surface method) computed by the GEM15 model was compared with the profile observations. Although the model agreed better with the observations in Lamont, it disagreed with the observations in Barrow by exhibiting a consistent positive bias and rapid unphysical oscillations. To circumvent this problem, an alternative profile method with a generalized constant was suggested for use in the GEM15 model based on the bulk Richardson number concept. This method worked well for both sites. In Barrow, it performed better than surface methods by reducing the MH bias by a factor of two. As a result, with this choice of MH parameterization, MH estimation in the GEM15 model may be improved without affecting other meteorological variables because MH is purely a diagnostic variable.

This study was focused on only two representative sites, among the few for which very rich surface and profile observations were available. The evidence provided here supports the idea that AQ modelling may benefit from an improved MH parameterization because MH is an important prognostic variable for this purpose. However, the real benefits will be known when such parameterizations are tested on an entire model domain. In a future study, the holistic impact of MH parameterization on the relevant AQ models will be assessed.

Acknowledgements

The authors are indebted to Hans Verlinde, Michael H. Liu, and Karen Gibson from the Atmospheric Radiation Measurement (ARM) program, Climate Research Facility, US Department of Energy, for advice on the retrieval of observational data for Lamont and Barrow. The lead author thanks Dr. David Tarasick, who inspired this study at its inception. Expert reviews by our colleagues Michael Moran, Paul Makar, Wanmin Gong, and Stephen Beagley are appreciated. The authors also acknowledge the constructive comments by reviewers of the journal who significantly contributed to the quality of the paper.

Funding

The funding support for this study was provided by Environmental Stewardship Branch, Energy and Transportation Directorate, Transportation Division, Environment Canada.

Disclosure statement

No potential conflict of interest was reported by the authors.

References

Anderson, P. S., & Neff, W. D. (2008). Boundary layer physics over snow and ice. *Atmospheric Chemistry and Physics*, *8*, 3563–3582. doi:10.5194/acp-8-3563-2008

AO, C. O., Waliser, D.E., Chan, S. K., Li, J-L., Tian, B., Xie, F., & Mannucci, A. J. (2012). Planetary boundary laver heights from GPS radio occultation refractivitv and humidity profiles. *Journal of Geophysical Research*, *117* (D16), D16117. doi:10.1029/2012JD017598

Arya, S. P. S. (1981). Parameterizing the height of the stable atmospheric boundary layer. *Journal of Applied Meteorology*, *20*(10), 1192–1202. doi:10.1002/qj.49710042507

Beyrich, F. (1997). Mixing height estimation from sodar data — A critical discussion. *Atmospheric Environment*, *31*(23), 3941–3953. doi:10.1016/S1352-2310(97)00231-8

Candlish, L. M., Raddatz, R. L., Asplin, M. G., & Barber, D. G. (2012). Atmospheric temperature and absolute humidity profiles over the Beaufort Sea and Amundsen Gulf from a microwave radiometer. *Journal of Atmospheric and Oceanic Technology*, *29*, 1182–1201. doi:10.1175/JTECH-D-10-05050.1

Dastoor, A., & Pudykiewicz, J. (1996). A numerical global meteorological sulfur transport model and its application to Arctic air pollution. *Atmospheric Environment*, *30*(9), 1515–1522. doi:10.1016/1352-2310(95)00243-X

Deardorff, J. W. (1972). Parameterization of the planetary boundary layer for use in general circulation models. *Monthly Weather Review*, *100*(2), 93–106.

Delage, Y. (1974). A numerical study of the nocturnal atmospheric boundary layer. *Quarterly Journal of the Royal Meteorological Society*, *100*(425), 351–364. doi:10.1002/qj.49710042507

Garratt, J. R. (1982). Observations in the nocturnal boundary layer. *Boundary-Layer Meteorology*, *22*(1), 21–48. doi:10.1007/BF00128054

Han, Z., Zhang, M., & An, J. (2009). Sensitivity of air quality model prediction to parameterization of vertical eddy diffusivity. *Environmental Fluid Mechanics*, *9*(1), 73–89. doi:10.1007/sl0652-008-9088-1

Helmig, D., Boylan, P., Johnson, B., Oltmans, S., Fairall, C., Staebler, R., … Shepson, P. (2012). Ozone dynamics and snow-atmosphere exchanges during ozone depletion events at Barrow, Alaska. *Journal of Geophysical Research*, *114*(D20), D20303.

Holtslag, A. A. M., & Boville, B. A. (1993). Local versus nonlocal boundary-layer diffusion in a global climate model. *Journal of Climate*, *6*(10), 1825–1842. doi:10.1175/1520-0442(1993)006<1825:LVNBLD>2.0.CO;2

Holtslag, A. A. M., De-Bruijn, E. I. F., & Pan, H.-L. (1990). A high resolution air mass transformation model for short range weather forecasting. *Monthly Weather Review*, *118*(8), 1561–1575.

Jakobsen, H. A., Berge, E., Iversen, T. & Skälin, R. (1995). *Status of the development of the multilayer Eulerian model EMEP/MSC-W Note 3/95* (Available from Norwegian Meteorological Institute) (Norwegian Meteorological Institute, Technical Report, P.O. Box 43, N-0313 Oslo 3, Norway).

Kitaigorodskii, S. A., & Joffre, S. M. (1988). In search of a simple scaling for the height of the stratified atmospheric boundary layer. *Tellus A*, *40A*(5), 419–433. doi:10.1111/j.l600-0870.1988.tb00359.x

Laroche, S., Gauthier, P., St-James, J., & Morneau, J. (1999). Implementation of a 3D variational data assimilation system at the Canadian meteorological centre. Part II: The regional analysis. *Monthly Weather Review*, *57*(3), 281–307. doi:10.1080/07055900.1999.9649630

Li, J., & Barker, H. W. (2005). A radiation algorithm with correlated-*k* distribution. Part I: Local thermal equilibrium. *Journal of the Atmospheric Sciences*, *62*, 286–309. doi:10.1175/JAS-3396.1

Lin, J.-T., Youn, D., Liang, X.-Z., & Wuebbles, D. J. (2008). Global model simulation of summertime U.S. ozone diurnal cycle and its sensitivity to PBL mixing, spatial resolution, and emissions. *Atmospheric Environment*, *42*(36), 8470–8483. doi:10.1016/j.atmosenv.2008.08.012

Liu, S., & Liang, X. Z. (2010). Observed diurnal cycle climatology of planetary boundary layer height. *Journal of Climate*, *23*(21), 5790–5809. doi:10.1175/2010JCLI3552.1

Mahrt, L. (1981). Modelling the depth of the stable boundary-layer. *Boundary-Layer Meteorology*, *21*, 3–19.

Mahrt, L. (1999). Stratified atmospheric boundary layers. *Boundary-Layer Meteorology*, *90*(3), 375–396. doi: 10.1023/A:1001765727956

Mahrt, L., & Vickers, D. (2006). Extremely weak mixing in stable conditions. *Boundary-Layer Meteorology*, *119*(1), 19–39. doi:10.1007/sl0546-005-9017-5

Mailhot, J., Bélair, S., Benoit, R., Bilodeau, B., Delage, Y., Fillion, L., … Tremblay, A. (1998). *Scientific description of RPN physics library - version 3.6* (Technical Report, Atmospheric Environment Service, Dorval, Quebec, Canada). Retrieved from http://colloboration.cmc.ec.gc.ca/science/rpn/physics/physic98.pdf

Mailhot, J., Bélair, S., Lefaivre, L., Bilodeau, B., Desgagné, M., Girard, C., … Qaddouri, A. (2006). The 15-km version of the Canadian Regional Forecast System. *Atmosphere-Ocean*, *44*(2), 133–149. doi:10.3137/ao.440202

Makar, P. A., Nissen, R., Teakles, A., Zhang, J., Zheng, Q., Moran, M. D.... diCenzo, C., (2014). Turbulent transport, emissions and the role of compensating errors in chemical transport models. *Geoscientific Model Development*, *7*, 1001–1024. doi:10.5194/gmd-7-1001-2014

Maryon, R. H., & Best, M. J. (1992). *'NAME', 'ATMES, and the boundary layer problem.* Met O (APR) turbulence and diffusion Note No. 204 (Technical Report, U. K. Met. Office, Exeter, Devon, U.K.).

Mason, P. J., & Thomson, D. J. (1987). Large-eddy simulations of the neutral-static-stability planetary boundary layer. *Quarterly Journal of the Royal Meteorological Society*, *113*(476), 413–443. doi:10.1002/qj.49711347602

McTaggart-Cowan, R., & Zadra, A. (2015). Representing Richardson number hysteresis in NWP boundary layer. *Monthly Weather Review*, *143*, 1232–1258. doi:10.1175/MWR-D-14-00179.1

Pollard, R. T., Rhines, P. B., & Thompson, R. O. R. Y. (1972). The deepening of the wind-mixed layer. *Geophysical Fluid Dynamics*, *4*(1), 381–404. doi:10.1080/03091927208236105

Richardson, L. F. (1920). The supply of energy from and to atmospheric eddies. *Proceedings of the Royal Society of London A*, *A97*, 354–373.

Rossby, C. G., & Montgomery, R. B. (1935). The layer of frictional influence in wind and ocean currents. *Papers in Physical Oceanography and Meteorology*, *3*(3), 1–101. doi:10.1575/1912/1157

Seibert, P., Beyrich, F., Gryning, S. E., Joffre, S., Rasmussen, A., & Tercier, P. (1998). *Mixing height determination for dispersion modelling* (COST Action 710. Final Report. Harmonization of the pre-processing of meteorological data for atmospheric dispersion models. L-2985 Luxembourg: European Commission, EUR 18195 EN (ISBN 92-828-3302-X)).

Seibert, P., Beyrich, F., Gryning, S. E., Joffre, S., Rasmussen, A., & Tercier, P. (2000). Review and intercomparison of operational methods for the determination of the mixing height. *Atmospheric Environment*, *34*(7), 1001–1027. doi:10.1016/S1352-2310(99)00349-0

Stull, R. B. (2003). *An introduction to boundary layer meteorology*. Dordrecht, Netherlands: Kluwer Academic Publishers.

Surridge, A. D., & Swanepoel, D. J. (1987). On the evolution of the height and temperature difference across the nocturnal stable boundary layer. *Boundary-Layer Meteorology*, *40*(1–2), 87–98. doi:10.1007/BF00140069

Tanguay, M., Fillion, L., Lapalme, E., & Lajoie, M. (2012). Four-dimensional variational data assimilation for the Canadian regional deterministic prediction system. *Monthly Weather Review*, *140*, 1517–1538. doi:10.1175/MWR-D-ll-00160.1

Taylor, G. I. (1935). Effects of variation in density on the stability of superimposed streams of fluids. *Proceedings of the Royal Society A: Mathematical, Physical and Engineering Sciences*, *132*(820), 499–523.

Vogelezang, D. H. P., & Holtslag, A. A. M. (1996). Evolution and model impacts of alternative boundary-layer height formulation. *Boundary-Layer Meteorology*, *81*, 245–269.

Wormington, M., Panaccione, C., Matney, K. M., & Bowen, D. K. (1999). Characterization of structures from X-ray scattering data using genetic algorithms. *Philosophical Transactions of the Royal Society A: Mathematical, Physical and Engineering Sciences*, *357*(1761), 2827–2848. doi:10.1098/rsta.l999.0469

Xie, F., Wu, D. L., Ao, C. O., Mannucci, A. J., & Kursinski, E. R. (2012). Advances and limitations of atmospheric boundary layer observations with GPS occultation over southeast Pacific Ocean. *Atmospheric Chemistry and Physics*, *12*, 903–918. doi:10.5194/acp-12-903-2012

Zilitinkevich, S. S. (1972). On the determination of the height of the Ekman boundary layer. *Boundary-Layer Meteorology*, *3*(2), 141–145. doi:10.1007/BF02033914

Zilitinkevich, S. S., & Baklanov, A. (2002). Calculation of the height of the stable boundary layer in practical applications. *Boundary-Layer Meteorology*, *105*(3), 389–409. doi:10.1023/A:1020376832738

Zilitinkevich, S. S., Baklanov, A., Rost, J., Smedman, A. S., Lykosov, V., L & Calanca, P. (2002). Diagnostic and prognostic equations for the depth of the stably stratified Ekman boundary layer. *Quarterly Journal of the Royal Meteorological Society*, *128*(579), 25–46. doi:10.1256/00359000260498770

Zilitinkevich, S. S., & Mironov, D. V. (1996). A multi-limit formulation for the equilibrium depth of a stably stratified boundary layer. *Boundary-Layer Meteorology*, *81*(3–4), 325–351. doi:10.1007/BF02430334